The structure of nonplanar molecular liquids: tetrachloroethylene

1989 J. Phys.: Condens. Matter 1 8595

(http://iopscience.iop.org/0953-8984/1/44/030)

J. Phys.: Condens. Matter 1 (1989) 8595–8607. Printed in the UK

The structure of non-polar molecular liquids: tetrachloroethylene

M Alvarez†, F J Bermejo†, P Chieux‡, E Enciso§, J Alonso† and N García§

† Instituto de Estructura de la Materia, Consejo Superior de Investigaciones Científicas, Calle Serrano 119, 28006-Madrid, Spain

‡ Institut Laue–Langevin, 156X BP 38042 Grenoble, France

§ Departamento Química Física, Facultad de Ciencias Químicas, Universidad Complutense, 28040-Madrid, Spain

Received 13 April 1989, in final form 5 June 1989

Abstract. A neutron diffraction study of liquid tetrachloroethylene (TCE) is presented. Analysis of the large-momentum-transfer part of the structure factor has enabled the refined intramolecular parameters to be found, and the departures from planarity on a quantitative basis to be discussed. The liquid short-range structure is discussed in terms of the site–site Ornstein–Zernike (SSOZ) integral equation which provides a way of decomposing the measured pair correlation function into its partial pair correlations.

1. Introduction

The way in which contributions such as molecular shape, polarisability and electrostatic multipolar interactions determine the structure and thermodynamics of real fluids remains a controversial topic [1].

Although, in principle, the liquid structure factors derived from radiation scattering experiments should be able to identify model interparticle potentials and, therefore, shed some light on this question, their sensitivity (needed to reveal details of fine structure) is very often diminished due to the complicated structure of the scattering (molecular) unit which dominates the diffraction pattern for momentum transfers greater than 3–4 $Å^{-1}$.

For dipolar fluids, contradictory results have been found. The apparent minimal contribution of electrostatic forces found in the case of acetonitrile [2] is being countered by recent findings on liquid sulphur dioxide [3] where the observed details of the $g(r)$ intermolecular pair correlation function can only be taken into account by introduction of unphysical energy parameters in the potential or by the use of additional terms which enhance the anisotropy of the intermolecular interaction.

In the case of liquids composed of non-dipolar molecules, the same trends have been reported. Here, the lack of importance of octupolar interactions in highly symmetric molecules like benzene [4] or carbon tetrachloride [5], is countered by the case of liquid

0953-8984/89/448595 + 13 $02.50

halogens [6] or even nitrogen [7], where substantial anisotropic contributions to the structure factor have been found.

In order to gain some insight into the origin of the short-range molecular correlations in the liquid phase, we have performed a study on liquid tetrachloroethylene (TCE), by means of neutron diffraction and integral equation approaches. The choice of this particular liquid was motivated by two reasons: on the one hand, it has a lower point group symmetry (V_h) than the previously studied compounds of this level of complexity (D_{6h} or T_d), and on the other hand, most of the scattering, intermolecular pattern is dominated by chlorine–chlorine correlations, thus making the study of short-range correlations more feasible. Because of the relative low weight of the carbon–carbon correlations, most of the contributions associated with the pair correlation function of the molecular centres are of small importance to the diffraction pattern. As a matter of fact, the final pair correlation function will be a mixture of the three components

$$g(r) = 0.066\, g_{CC}(r) + 0.383\, g_{C\text{-}Cl}(r) + 0.551\, g_{ClCl}(r) \tag{1}$$

where the scarce importance of the $g_{CC}(r)$ function can be seen.

2. Experimental procedure and corrections

The static single-differential cross section was measured on the D4B diffractometer at one of the hot lines of the high flux reactor of the Institut Laue-Langevin, Grenoble, France, using an incident wavelength of 0.4989 ± 0.0005 Å (calibrated with a nickel powder standard). A thin-walled vanadium container (0.470 cm ID, 0.51 cm OD) was filled with the sample and the experiment was performed by recording the count distribution in the 1.65°–140° angular range at room temperature. The absorption (self-attenuation) corrections were evaluated by means of the usual Paalman–Pings formalism [8]. The attenuation coefficients evaluated by this formula were found to be $A_{s,sc} = 0.740$, $A_{c,sc} = 0.838$ and $A_{c,c} = 0.994$, where the subscripts s, sc and c stand for sample, sample and container, and container, respectively.

Data normalisation was achieved using a vanadium rod standard following the usual procedure [9].

The correction for multiple-scattering was calculated by means of a Monte Carlo code [10] which yields an angular average of multiply scattered neutrons of 11.6%. The contribution corresponding to multiply scattered neutrons was subtracted afterwards using standard procedures [9].

In order to evaluate the relative importance of the inelastic component to the observed, total cross section, several preliminary calculations were performed. The first step consisted in the computation of bounds to the value of the mass of the recoiling particle. The low-energy bound was obtained by means of computation of the Sachs–Teller tensors [11] for every nucleus. For such a purpose, the individual molecular geometry by gas-phase electron diffraction (ED) was taken [12]. The effective masses (M_{eff}) computed from the trace of the inverse-mass tensor, were found to be $M_{eff}^{C} = 150.88$ amu for each carbon nuclei and $M_{eff}^{Cl} = 77.13$ amu for each chlorine. On the other hand, the free-particle limit, computed from the atomic weights and total cross sections of the nuclei was 34.26 amu.

It was found that the slight fall-off of the cross section at large angles could be easily accounted for in terms of a simplified generalised Placzek expression [13] of the type

$$\left.\frac{\mathrm{d}\sigma}{\mathrm{d}\Omega}\right|_{\text{self}} = \left(\sum_i b_i^2 + \frac{\sigma_i^{\text{inc}}}{4\pi}\right) P(Q, \lambda_0) \tag{2}$$

where b_i and σ_i stand for nuclear scattering lengths and incoherent cross section, respectively, and the term containing the inelasticity contribution was found to be

$$P(Q, \lambda_0) = 1 + CQ^2 = 1 + (\alpha_d / M_{\text{eff}})(\lambda_0 / 4\pi)^2 \tag{3}$$

where α_d represents a detector constant ($\alpha_d \simeq 3.27$ for the present measurement) and M_{eff} was taken as a free parameter whose value was obtained by means of a parametric fit. A value of $M_{\text{eff}} \simeq 77$ amu, adequately represented the fall-off.

The highest vibrational frequency of this molecule corresponds to an A_{1g} mode [14] which combines C–C and C–Cl bond stretches with a bond-angle deformation. Such excitation occurs at 1571 cm^{-1} which is far below the incident neutron energy ($E_0 \simeq$ 2663 cm^{-1}). Although such radiation can excite the internal molecular modes the fact that the principal moments of inertia are large enough (I = 669, 375, 294 amu Å^2) allows us to assume that such excitations are uncorrelated with the rotational motions. This experimental condition correspond to regime II considered by Egelstaff [15] where the analysis of the high-angle portion of the differential cross section may be carried out using simplified formulas.

As a check on the normalisation applied to the data, the quantity $S(0)$ (i.e. the measured, normalised structure factor extrapolated a zero-angle) was computed, from which an isothermal compressibility $\chi_T = 7.56 \times 10^{-10}\ \text{m}^2\ \text{N}^{-1}$ was obtained. The resulting corrected cross section is shown in figure 1.

3. Data analysis

The structure factor for a molecular fluid is given by

$$S(Q) = \frac{1}{N}\left[1\Big/\left(\sum_i b_i\right)^2\right]\left\langle \sum_{ij} b_i b_j \exp(\mathrm{i}\boldsymbol{Q}\cdot\boldsymbol{r}_{ij})\right\rangle = \left[1\Big/\left(\sum_i b_i\right)^2\right]\frac{\mathrm{d}\sigma}{\mathrm{d}\Omega_{\text{coh}}} \tag{4}$$

where the b_i denote coherent scattering amplitudes and the angular brackets stand for a thermal average. The structure factor can be decomposed into a contribution due to scattering from single molecules $f_1(Q)$ and a function $D_m(Q)$ which comprises all the intermolecular information.

In our case the $f_1(Q)$ contains six different terms and the $D_m(Q)$ function is a transform of the $g(r)$ given by equation (1), so that

$$D_m(Q) = 4\pi\rho \int_0^\infty [g(r) - 1]\, j_0(Qr) r^2\, \mathrm{d}r \tag{5a}$$

and

$$f_1(Q) = \left[1\Big/\left(\sum_i b_i\right)^2\right]\left[\sum_{ij} b_i b_j j_0(Qd_{ij}) \exp\left(\frac{-Q^2 x_{ij}^2}{2}\right)\right] \tag{5b}$$

where $j_0(x) = (\sin x)/(x)$, and x_{ij}^2 represents the mean-square atomic displacement.

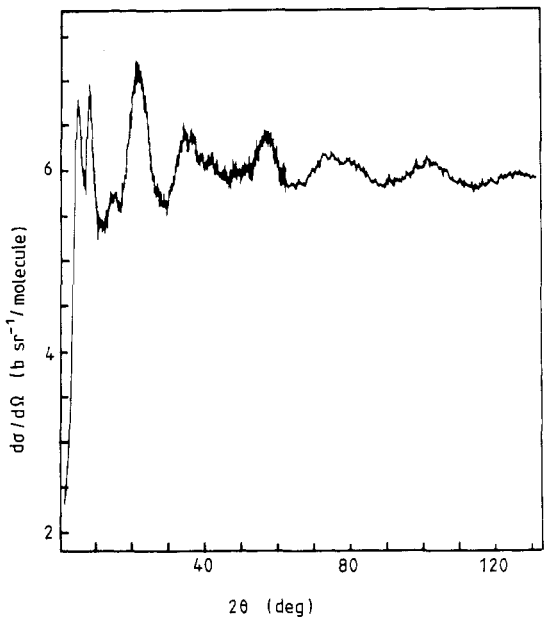

Figure 1. The measured neutron single-differential cross section, after correction for absorption and multiple scattering.

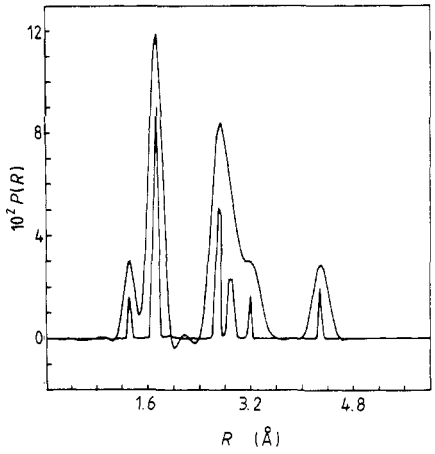

Figure 2. Intramolecular distance probability functions $P(R)$. The upper trace corresponds to the Fourier–Bessel transform of the molecular form factor $i(Q)$. The lower curve represents the ME inversion of the high-Q portion of the molecular structure factor, multiplied by 0.5.

The oscillatory part at high-Q obtained after subtraction of the self-scattering terms from $f_1(Q)$ may be written as

$$Qi(Q) = \sum_{i \neq j} b_i b_j j_0(Qd_{ij}) \exp\left(\frac{-Q^2 x_{ij}^2}{2}\right) = Q\left[f_1(Q) - \sum_i b_i^2\right]. \tag{5c}$$

The Fourier–Bessel transform of this reduced intensity function will give the intramolecular distances probability distribution

$$d_m(r) = \frac{2}{\pi}\left[\left(\sum_i b_i\right)^2 \Big/ \sum_i b_i^2\right] \int_0^\infty Qi(Q) \sin Qr \, dQ \tag{6}$$

so that all the structural correlations can be decomposed as a sum of intramolecular $d_m(r)$ and $d_l(r)$, or liquid structure parts:

$$d(r) = d_m(r) + d_l(r) \tag{7}$$

where $d(r)$ is the transform of the full intensity function (containing the intermolecular contributions $D_m(Q)$).

The separation of the intra- and intermolecular contributions can only be safely applied if they are well separated in real (direct) space. To check the extent of overlap between both contributions an inversion of the high-Q portion of the structure factor was performed by means of a maximum entropy (ME) treatment described elsewhere [16]. The resulting ME map is shown in figure 2. As can be seen upon inspection of the

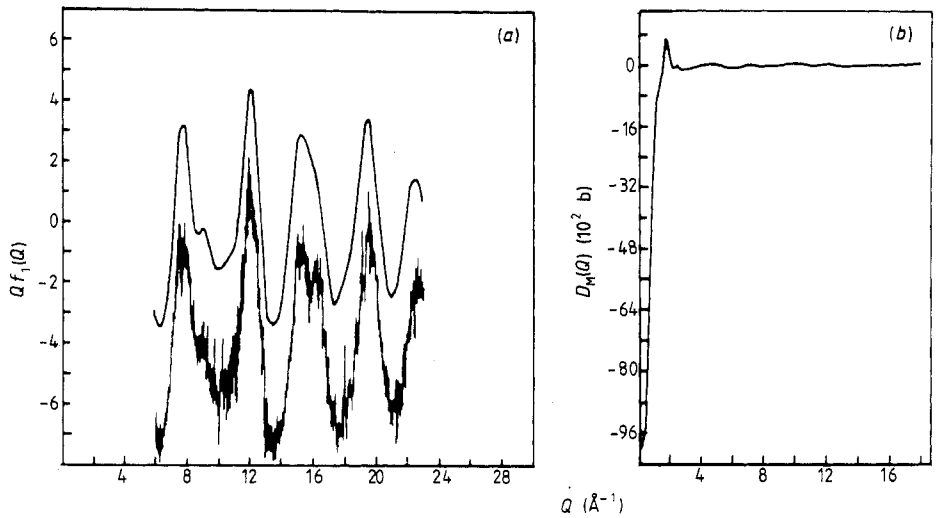

Figure 3. (*a*) The optimal molecular form factor fit (upper curve) to the measured $QS(Q)$ reduced intensity function (lower trace). (*b*) The derived intermolecular structure factor obtained by subtraction of the $f_1(Q)$ from the reduced intensity function.

figure, the six intramolecular components, are well resolved and the corresponding internuclear distances are given in table 1. A brief comparison with the gas-phase (ED) data reveals that the possible contributions of inelasticity effects to the interference contribution have to be small, thus justifying the simplified approach herein described.

In order to get a set of refined values for the intramolecular parameters, a fit of a $f_1(Q)$ function to the high-Q portion of $S(Q)$ was performed.

All the observed features were adequately taken into account using the sum of six contributions given by equation (6). The intramolecular distance probability density curve is given in figure 2 and compared to the ME counterpart. The fitted form-factor $f_1(Q)$ is shown in figure 3(*a*) and the $D_m(Q)$ intermolecular function in figure 3(*b*).

The numerical data corresponding to d_{ij} distances and 'effective' mean-square amplitudes of vibration are given in table 1.

As can be seen from table 1 both sets of distances agree within the experimental error with the one derived from the gas-phase study. However, small but significant differences between the distances corresponding to the ME set and those from ED or parametric $f_1(Q)$ fits to $S(Q)$ are found.

It should be recalled that the internuclear distances coming from this experiment correspond to thermal average values taken over a set of vibrational states. It should be taken into account that the molecule is substantially excited at room temperature. A rough measure of the degree of thermal excitation is given by the quantity $g_\nu = \coth(h\omega_\nu/2k_BT)$ where ω_ν is the vibrational angular frequency and k_B is the Boltzmann constant. For values of $g_\nu > 1.0$ substantial thermal excitation takes place and, therefore, terms corresponding to higher order vibrational states will contribute to the cross section. A quick estimate of these effects can be made computing the values of the quantities

$$Vg_\nu = (hQ^2/4M_{\text{eff}}\omega_\nu)\, g_\nu \tag{8}$$

Table 1. Intramolecular parameters for TCE (Distances are in angströms, angles in degrees. The quantities given in brackets are standard deviations.)

Parameter	ME map[a]	Electron diffraction[b]	$f_1(Q)_{fit}$[c]	x_{ij}[b,d]	x_{ij}[c,d]	Coordinate[e]	g[f]	Vg^g_ν
d_{C-C}	1.310 (23)	1.30 (3)	1.311 (51)	0.030 (assumed)	0.0203 (525)	Q(C–C) (A_{1g})	1.00	0.22
d_{C-Cl}	1.706 (12)	1.72 (1)	1.715 (47)	0.048 (5)	0.0262 (485)	Q(C–Cl) (A_{1g}, B_{1g}, B_{2n}, B_{3n})	1.24	0.43
$d_{C\cdots Cl}$	2.687 (17)	2.66 (2)	2.671 (36)	0.058 (10)	0.0486 (500)	γ(CCCl), γ(ClCCl)	1.55	0.63
$d_{Cl\cdots Cl}$	2.901 (10)	2.88 (1)	2.873 (43)	0.070 (10)		γ(CCCl), γ(ClCCl)		
$d_{Cl\cdots Cl}^{cis}$	3.169 (18)	3.17 (2)	3.189 (48)	0.125 (10)	0.1543 (610)	γ(CCCl), γ(ClCl)(B_{1g}, B_{3n})	3.76	0.85
						ρ_{CCl_2}, $\chi^{CCl_2}_{CCl_2}$(A_{1n}, A_{1n})		5.17
$d_{Cl\cdots Cl}^{trans}$	4.294 (09)	4.29 (2)	4.290 (39)	0.086 (10)	0.0585 (575)	ρ_{CCl_2}, $\chi^{CCl_2}_{CCl_2}$(B_{1n}, A_{1n})		
ClĈCl	112.35 (1.3)	113.5 (1.5)	113.47 (0.06)					
ClĈC	125.47	123.25	123.26					

[a] Computed by means of a decomposition of $P(R)$ of figure 2, as a sum of six gaussians.
[b] Taken from [12].
[c] Computed by fitting (16) to the $4 \leq Q \leq 24$ Å^{-1} region of $S(Q)$.
[d] Units: Å.
[e] The assignment is taken from [14]: the $Q(x)$ are bond stretches; the γ are bond-angle bendings, the ρ_{CCl_2} are out-of-plane bendings and the χ correspond to torsional oscillations about the C=C bond. The symmetry species involved are given in brackets; molecular symmetry belongs to the V_h point group.
[f] Computed using the tabulated frequencies given in [14].
[g] Computed using (7) for $Q = 22$ Å^{-1}.

where M_{eff} is a ratio between atomic masses, and will be identified with the Sachs–Teller masses since they constitute an upper limit for the effective mass for first-order scattering.

As an indication values of the dimensionless quantities Vg_ν are given in the last column of table 1. As can be seen, all modes corresponding to internuclear distances different from the C–C bond length can contribute to the observed cross section at large scattering angles. Such a fact can explain the slightly short C–Cl bond distance obtained from the decomposition of the ME map.

On the other hand the long Cl . . . Cl distances computed from the local geometry defined by the C–C, C–Cl bond lengths and Cl–C–Cl bond angle are about 0.04 Å larger than those computed assuming a planar molecule. Those kind of discrepancies can be explained taking into account the existence of three vibrational out-of-plane modes of symmetries B_{2g}, B_{1u} and A_{1u} corresponding to symmetric and antisymmetric out-of-plane motions and torsional oscillations about the C–C bond, respectively.

Since no complete (including anharmonic constants) force field for this molecule is available, a rigorous derivation of the atomic cartesian displacements for all atoms cannot be performed. However, an empirical estimate of the magnitude of this displacement may be obtained from either Taylor series expansion of the distances through the quadratic terms of the displacements or from procedures which follow the work of James [17] half a century ago. In particular, the short-distance part of the total interference function $d_m(r)$ (with $0 \leqslant r \leqslant 5$), can be separated from the total transform on the following grounds:

(i) assume that all distances pertaining to atoms separated by one or two bonds give rise in the transform to a sum of gaussians, one for every pair of atoms with equilibrium

$$t(r) = \frac{\pi}{2} \sum_{i \neq j} b_i b_j \exp\left|\frac{-(d_{ij} - r)^2}{4\gamma_{ij}}\right| \tag{9}$$

positions $d_i d_j$ and mean-square amplitudes of vibration $\gamma = -\frac{1}{2}(\chi_{ij})^2$.

(ii) for the distances between atoms separated by three bonds, their transform was taken to be [12]

$$t'(r) = (\pi C/4A)(\beta h^{1/2}/2l_2)^{1/2}/(1 - E_1)^{-1/2} \exp[-4(r - l_2)/(4h + 1)]\,|q_1|^{1/2} \times \exp(\tfrac{1}{2}q_1^2) \begin{cases} I_{-1/4}(q_1^2/2) + I_{1/4}(q_1^2/2) & q_1 \geqslant 0 \\ I_{-1/4}(q_1^2/2) - I_{1/4}(q_1^2/2) & q_1 < 0 \end{cases} \tag{10}$$

where l_2 is the equilibrium distance (maximum for atoms located in the trans position), $I_{1/4}$ are Bessel functions of fractional order

$$\beta = 4K/k_B T(l_2^2 - l_1^2) \tag{11}$$

where K is the force constant of the (simplified) potential hindering internal rotation and l_1 is the equilibrium distance for the pair of atoms in *cis*-position. The remaining symbols are

$$\begin{aligned} q_1 &= [l_2 h(1 - 4\beta) - r(h + \beta)/(4h + 1)^{1/2}[h(4h + 1) - 4(h + \beta)^2]^{1/2} \\ 1 - E_1 &= h(4h + 1) - 4(h + \beta)^2/h(4h + 1) \\ A &= [(4h + 1)/4]^{1/2} \end{aligned} \tag{12}$$

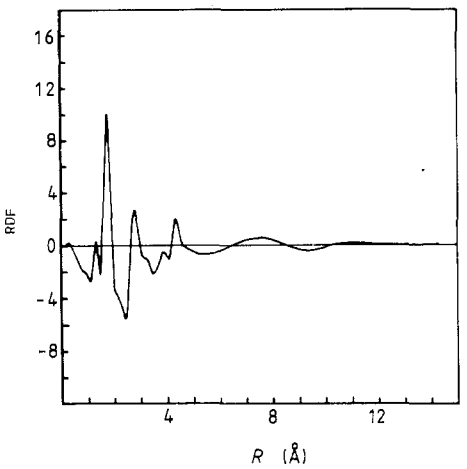

Figure 4. The total pair correlation function $d(r)$ computed using (14). The derived number density $\rho_0 = 5.9 \times 10^{-3}$ mol Å^3.

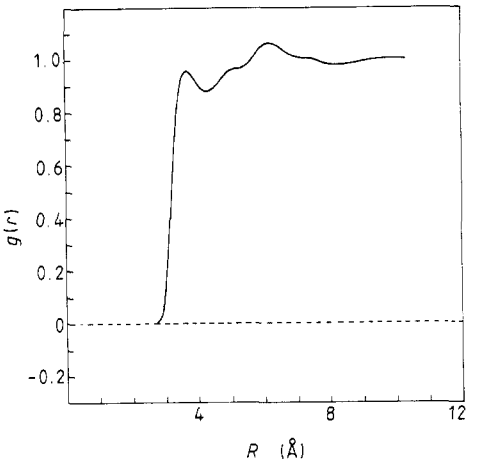

Figure 5. The intermolecular pair correlation function $g(r)$ obtained by inversion of the structure factor $D_m(Q)$.

where $2h = 1/(x_{ij}^2)$ and x_{ij} is the mean-square displacement of the pair i–j. The total molecular distance probability distribution can then be decomposed into a sum of Gaussians, $t(r)$ and a sum of distorted gaussian functions $t'(r)$. Equation (10) thus provides a way to estimate the strength of the hindering potential

$$V_\varphi = K\varphi^2 \tag{13}$$

which, although only valid for small displacements, will enable us to assess the effect of out-of-plane vibrations on the interatomic distances.

4. Liquid structure

As a first step in the analysis of the static, intermolecular pair correlation function $g(r)$, the differential function

$$d_1(r) = 4\pi r\rho[g(r) - 1] \simeq \frac{2}{\pi}\int_0^{Q_{max}} QD_m(Q)\sin(Qr)\,dr \tag{14}$$

was evaluated by means of a standard quadrature procedure, and the resulting function is shown in figure 4. As can be readily seen from the figure the short-range structure of $d(r)$ shows a first sharp peak located at $\simeq$3.8 Å and a complex, broad structure, centred at $\simeq$7.5 Å. Contrary to most usual liquids, there are no noticeable oscillations after about 10 Å.

The intermolecular structure factor derived by subtraction of the molecular part

$$D_m(Q) = S(Q) - f_1(Q) = \frac{4\pi\rho}{Q}\int_0^{\infty} r[g(r) - 1]\sin(Qr)\,dr \tag{15}$$

is shown in figure 3(b).

The relevant $g(r)$, intermolecular pair correlation function computed using a previously described scheme [15] is shown in figure 5.

5. SSOZ integral equation predictions

5.1. The SSOZ integral equation

The site–site radial distribution function $g_{\alpha\beta}(r) = h_{\alpha\beta}(r) - 1$ can be defined by solution of an Orstein–Zernike (OZ)-like equation [18] written in matrix form as

$$\mathbf{h} = \mathbf{w} \otimes \mathbf{c} \otimes \mathbf{w} + \rho \mathbf{w} \otimes \mathbf{c} \otimes \mathbf{h} \tag{16}$$

which we will refer to as the site–site Ornstein–Zernike (SSOZ) equation [19]. Here, $\otimes$ means convolution, **h** and **c** are the site pair labelled matrices of the total and direct site–site correlation functions, **w** is the corresponding matrix of intramolecular site–site correlation functions, and ρ is the molecular number density. The intramolecular pair distribution function is obtained by

$$w_{\alpha\beta}(r) = (1 - \delta_{\alpha\beta})(4\pi l_{\alpha\beta})^{-1}\, \delta(r - l_{\alpha\beta}) \tag{17}$$

where the distance between site α and β within the same molecule is a constant $l_{\alpha\beta}$. Other approximations needed for applying this theoretical scheme make it unnecessary to consider better descriptions for the ensemble average of these intramolecular correlations. The main approximation is based on the definition of a closure relation for $c_{\alpha\beta}(r)$, similar to the one used in the OZ equation. Several heuristic closures, coming from the Percus–Yevick and hypernetted chain (HNC) [20], have been widely applied.

According to the HNC closure we can define in terms of the site–site correlation functions the following relation

$$c_{\alpha\beta}(r) = \exp[-\beta u_{\alpha\beta}(r) + \gamma_{\alpha\beta}(r)] - \gamma_{\alpha\beta}(r) - 1 \tag{18}$$

where $\gamma_{\alpha\beta}(r) = h_{\alpha\beta}(r) - c_{\alpha\beta}(r)$, and $\beta = 1/k_B T$. Some criticisms have been made about such extension [21], but the short-range structural information (i.e. a few diameters of atomic separation) agree in a quantitative way with simulation results. The SSOZ integral equation is thus an adequate tool for obtaining a first description on the atomic arrangement in the liquid regime. Usually it is implemented with fast numerical algorithms, like the Gillan's method [22].

5.2. Intermolecular force models

The neutron diffraction patterns can be used in an inductive scheme to understand the intermolecular forces that are present between molecules in the liquid regime. For matching such information the intermolecular interactions are usually modelled by site–site pair interactions [2]. For small non-associated molecules like halogens [6] or sulphur dioxide [3] the neutron diffraction data have been used for discriminating some of the models proposed, although several of them can account for the thermodynamic properties of these liquids. When the number of atomic species increase in the molecular unit, the present-day accuracy of the neutron experiments can only give us coarse information on the intermolecular forces [5]. After data analysis we obtain an average description of the atom–atom radial distributions, each one showing a different length

Table 2. Model potential parameters and coherent neutron scattering lengths (in fermis, i.e. 10^{-15} m).

Model	ε/K (K)	σ (A)	$q(e)$[a]	$\bar{b}_N$ (fm)
Cl A[b]	120	3.40	—	9.5792
Cl B[c]	147	3.36	−0.1	
C A[b]	39	4.60	—	6.6484
C B[c]	51	3.35	+0.2	

[a] In units of the charge on an electron.
[b] Taken from [24].
[c] Taken from [23].

scale which makes it difficult to decompose the experimental information into the respective partials. According to this, for TCE we have used a flexible site–site Lennard–Jones (LJ) equation plus point charge interactions given as shown below,

$$U(1,2) = \sum_{\alpha}\sum_{\beta} 4\varepsilon_{\alpha\beta}\left|(\alpha_{\alpha\beta}/r_{\alpha\beta})^{12} - (\alpha_{\alpha\beta}/r_{\alpha\beta})^{6}\right| + \sum_{\alpha}\sum_{\beta}\frac{q_\alpha q_\beta}{r_{\alpha\beta}} \qquad (19)$$

and defined with a small number of parameters. The parameters ε and α denote the well depth and the diameter, respectively, of the corresponding LJ potential, and the q are the partial charges fixed on each site. The charges were obtained according to the electrostatic charge distribution computed using a semi-empirical molecular orbital calculation, which gives a long-range quadrupolar moment of $\theta_{xx} = -0.42$, $\theta_{yy} = -0.41$ and $\theta_{zz} = 0.83$, given in units of $e\text{Å}^{-2}$. The LJ parameters were chosen according to the standard parameters for this atomic species that exists in the literature [23, 24]. The numerical values of the potential parameters are given in table 2. Model A was considered first since it was used for theoretical studies of liquid Cl_4C [22, 5]. The comparison of both sets of radial distribution functions will show the influence of different intramolecular atomic arrangements on the liquid structure. The geometric parameters, bond lengths distances and angles, are fixed to the average values obtained in the previous data analysis of the intramolecular contributions to the structure factor.

6. Results and discussion

6.1. Intramolecular structure

The intramolecular parameters of TCE obtained from ME analysis and from molecular form-factor fits to the high-Q portion of the structure factor are given in table 1. The quantities listed as X_{ij} correspond to RMS amplitudes of vibration projected on the lines connecting pairs of atoms at equilibrium. Most of the values found for the intramolecular distances agree quite well with gas-phase ED data [12]. The most noticeable feature was the large vibrational amplitude of the $d_{Cl\ldots Cl}$ distance (0.15 Å^2). Such a fact, previously found in ED experiments has been discussed in terms of departures from coplanarity arising from a twist on the C–C angle (about 15°) or a bend locating the carbon atoms above and below the plane containing the four chlorines [14]. As pointed out in previous sections there exist three low-frequency out-of-plane modes which should be substan-

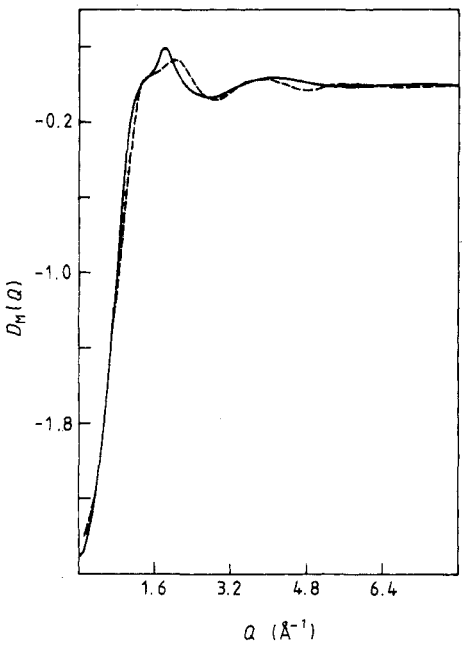

Figure 6. Intermolecular structure factors $D_m(Q)$. The full curve shows the experimental results. The broken curve gives the result obtained from the solution of the SSOZ integral equation.

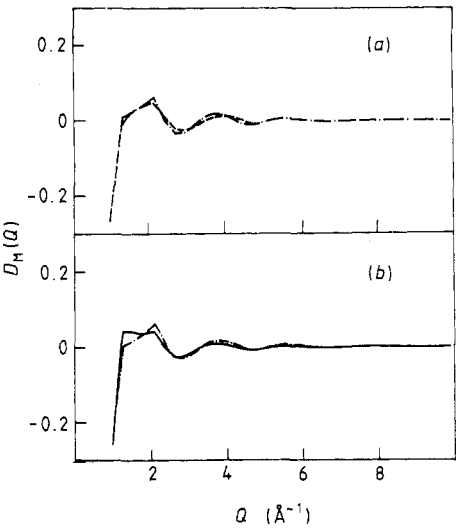

Figure 7. The SSOZ intermolecular structure factor $D_m(Q)$ for TCE obtained using different pair correlation models. (*a*) The effect of electrostatic forces on the liquid structure. The broken curve represents results for model B and the chain curve gives the results corresponding to the uncharged model. (*b*) The effect of short-range forces on the liquid structure factor. The chain curve represents results for model B (uncharged) and the full curve gives the results computed using model A.

tially excited at room temperature. The value found for the force constant K of equation (13) was 4.3×10^{-19} J rad^{-2}. Using such a value and employing a classical approximation, the $X_{Cl\ldots Cl}$ displacement corresponding to the lowest-lying, out-of-plane frequency ($h\omega_\nu \simeq 13$ meV), can be computed from

$$X_{Cl\ldots Cl} = \tfrac{1}{2}|(h\omega_\nu/K)\coth(h\omega_\nu/2k_BT)|$$

giving an estimated value of $X_{Cl\ldots Cl} \cong 0.10$ Å. Such a value would correspond to an oscillation about the central bond of about 10°, or an out-of-plane displacement of less than 5°, or a combination of both types of motion.

6.2. *Liquid structure*

The intermolecular structure factor can be written as

$$D_m(Q) = 4\bar{b}_C^2 a_{CC}(Q) + 16\bar{b}_{Cl}b_C a_{CCl}(Q) + 16\bar{b}_{Cl}^2 a_{ClCl}^2(Q) \tag{20}$$

with partial structure factors defined by

$$a_{\alpha\beta}(Q) = \int_0^\infty \exp(-i\boldsymbol{Q}\cdot\boldsymbol{r})\rho h_{\alpha\beta}(r)\,dr \tag{21}$$

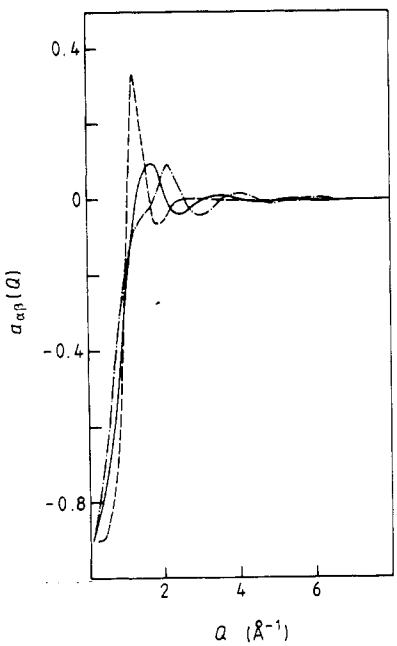

Figure 8. The SSOZ intermolecular partial structure factors $a_{\alpha\beta}(Q)$ of TCE computed using model B. Full, broken and chain curves correspond to the functions $a_{CCl}(Q)$, $a_{CC}(Q)$ and $a_{ClCl}(Q)$ respectively.

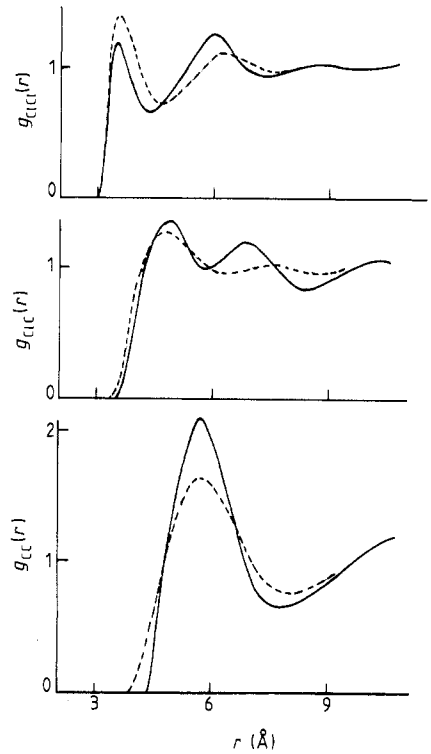

Figure 9. The SSOZ predicted partial pair correlation functions $g_{\alpha\beta}(r)$ computed using model A (broken curves) compared with the results obtained for liquid CCl_4 (full curves).

and the numerical values for the coefficients given in equation (1). The agreement between the theoretical predictions from model B and the experimental structure factor is shown in figure 6. For low Q-values the theory is unable to predict the correct compressibility limit, since it gives values for $D_m(0)$ that are too large. Such difficulties in predicting the long-range liquid structure are a well known characteristic of the approximation used here [21].

The influence of the electrostatic interactions upon the function $D_m(Q)$ is illustrated in figure 7. As can be seen, such an effect has to be small and in the present measurement it becomes comparable with the experimental uncertainty. Such an effect manifests itself in a change in the intensity of the first peak for the uncharged models. Model B gives a better overall agreement than model A. As an illustration of the behaviour of the three partial functions, figure 8 shows the partial structure factors computed for model A. Both correlations involving chlorine show an oscillatory behaviour with a small phase shift between them which gives rise to low-amplitude oscillations in the resulting $D_m(Q)$.

For the purposes of comparison, it is instructive to see how the rather different atomic arrangements corresponding to molecules formed by the same species, Cl_4C and Cl_4C_2 influence the liquid structure. In the first case, carbon tetrachloride, the tetrahedral arrangement allows more contacts between chlorine atoms than the ones in TCE. As a consequence of the planar structure of this molecule the partial $g_{ClC}(r)$ function

does not show any significant structure beyond the first peak, a fact which is countered by liquid Cl_4C [5].

The results presented in this work provide some estimation about the requirement in signal-to-noise ratios necessary to derive relevant information for the liquid structure of systems consisting of molecular species of complexity beyond diatomics (6). The subtle changes in intensity produced by the electrostatic interactions imply that a statistical counting precision near the limit of present day sources (about 1%) would be required to perform an evaluation of the role of such intermolecular forces.

Acknowledgments

This work was supported by grant no PB86-0617-CO2 of the CICYT (Spain). Excellent technical support for the preparation of the manuscript was given by Mr L de la Vega and A Gómez.

References

[1] See Rossky P J 1985 *Ann. Rev. Phys. Chem.* **36** 321
See Caillol J M, Levesque D, Weiss J J and Patey G N 1987 *Mol. Phys.* **62** 1225
[2] Hsu C S and Chandler D 1979 *Mol. Phys.* **36** 215; 1979 *Mol. Phys.* **37** 299
Chandler D 1982 *The Liquid State of Matter* ed. E W Montroll and J L Lebowitz (Amsterdam: North-Holland)
[3] Alvarez M, Bermejo F J, Chieux P, Enciso E, García-Hernández M, García N and Alonso J 1989 *Mol. Phys.* **66** 397
[4] Evans D J and Watts R O 1976 *Mol. Phys.* **32** 93
[5] Bermejo F J, Enciso E, Alonso J, García N and Howells W S 1988 *Mol. Phys.* **64** 1169
[6] Rodger P M, Stone A J and Tildesley D J 1988 *Mol. Phys.* **63** 173
[7] Street W B and Tildesley D J 1986 *Proc. R. Soc.* A **348** 485
Few G F and Rigby M 1977 *Mol. Phys.* **33** 585
[8] Paalman H H and Pings C J 1962 *J. Appl. Phys.* **33** 2635
[9] See for instance Bertagnolli H, Chieux P and Zeidler M D 1976 *Mol. Phys.* **32** 759
[10] Meardon B H 1973 *AERE Report* R7307
[11] Sachs R G and Teller E 1941 *Phys. Rev.* **60** 18
[12] Karle I L and Karle J 1952 *J. Chem. Phys.* **20** 63
[13] Powles J G 1979 *Mol. Phys.* **37** 623 and references therein
[14] Sverdlov L M, Korner M A and Krainov E P 1971 *Vibrational Spectra of Polyatomic Molecules; Israel Programme for Scientific Translations* (New York: Wiley) p 407
[15] Egelstaff P A and Soper A K 1980 *Mol. Phys.* **40** 569
[16] Bermejo F J, Santoro J, Mompean J and Dore J C 1987 *Nucl. Instrum. Methods* B **28** 135
[17] James R W 1932 *Z. Phys.* **33** 437
Karle J 1981 *Diffraction Studies on Non-crystalline Substances* ed. I Hargittai and W J Orville-Thomas (Budapest: Akademiai Kiadó)
[18] Chandler D and Andersen H C 1972 *J. Chem. Phys.* **57** 1930
[19] Stell G, Patey G N and Hope J S 1981 *Adv. Chem. Phys.* **48** 183
[20] Hansen J P and McDonald I R 1986 *Theory of Simple Liquids* 2nd edn (New York: Academic)
[21] Cummings P T, Gray C G and Sullivan D E 1981 *J. Phys A: Math. Gen.* **14** 1483
[22] Gillan M J 1979 *Mol. Phys.* **38** 1781
Enciso E 1985 *Mol. Phys.* **56** 129
[23] Mountain R D and Morrison G 1988 *Mol. Phys.* **64** 91
[24] Serrano F, Bañon A and Santamaría J 1984 *Chem. Phys. Lett.* **107** 475